The stabilising effect of oxides in foamed aluminium alloy scrap

G. S. Vinod Kumar[1,4*], F. García-Moreno[1,2], J. Banhart[1,2], A. R. Kennedy[3]

1. Technische UniversitätBerlin, Hardenbergstraße 36, 10623 Berlin, Germany

2.Helmholtz ZentrumBerlin, Hahn-Meitner-Platz 1, 14109 Berlin, Germany

3. University of Nottingham, Nottingham, NG2 7RD, UK

4. SRM Research Institute, SRM University, Kattankulathur, 603203, India

Abstract

The expansion and stability of foams made from remelted aluminium alloy scrap has been studied by in-situ X-ray radioscopy. Foams made from scrap alloy contain oxide bi-films introduced from the swarf and these oxides act as stabilizing agents. The wettability of the oxides and hence the stabilisation is studied by varying the addition of Mg (0 to 2 wt.%) in the alloy. The viscosity of the melts with and without Mg addition is measured and correlated with foam expansion and stability. A detailed microstructure analysis of the base alloy and foam cell wall was conducted to obtain an understanding of the stabilisation behaviour of oxides.

Keywords: Closed cell foams, Scrap alloy, Stabilisation, Aluminium, X-ray radioscopy

1. Introduction

Making closed-cell aluminum alloy foams directly from molten alloys offers a low cost route, as fewer processing steps are required compared to manufacturing from metal powders[1-2], but necessitates the introduction of ceramic or intermetallic particles for foam stabilisation[3-5].Ceramic particles such as SiC, Al_2O_3, TiB_2, TiC [6,7] and $MgAl_2O_4$[8] have been found to be effective stabilizing agents for aluminum foams but the introduction of these (sometimes expensive) particles into the matrix requires additional processing steps.

* Corresponding author ; vinodnarasimha@gmail.com

Making aluminium foams entirely from scrap is attractive due to the cost savings offered by a low-cost matrix and the potential for eliminating expensive foam-stabilising additives. For particular alloys, sourced carefully, reproducibility in form, composition and cleanliness can be achieved, in quantities that are commensurate with those required for niche products such as Al foams. For Al in the form of chippings or turnings from machining processes, powder metallurgy (PM) or liquid routes (analogous to the Alulight or Alporas methods, respectively) to make metal foams could be adopted. In reality, alloy turnings have high aspect ratios, pack very poorly and have low compressibility, making foamable precursors difficult to be manufactured by PM, favouring foam production via a liquid route. Despite this, Kanetake et al.[9] have been successful in making foams from metal chips by a powder route albeit by laborious (and no doubt expensive) multi-step compressive and torsional consolidation processes followed by extrusion.

Remelted Al scrap in the form of used beverage cans, has been used [10] in conjunction with TiH_2 blowing agent to produce Al foam. It is reported that the scrap, via the oxides introduced from their surfaces, acts as a viscosity thickener, aiding foaming [10]. Highly distorted cell structures were, however, observed and attributed to the inhomogeneous distribution of the introduced oxides. Although it was concluded that the agglomerated oxide particles introduced could not act as a foam stabiliser, subsequent development has led to commercial exploitation of this process by Foamtech with a product under the trade name LASOM^{TM}. Alcoa also report the development of an Al foam derived from scrap material made by a liquid route using $CaCO_3$ as a foaming agent [2] and Haesche et al. have utilised thixocasting to produce foamable precursors from a combination of alloy chips(AlSi9Cu3 and AlMg4.5Mn) and either a $CaCO_3$ or $CaMg(CO_3)_2$foaming agent [11].Further they added 3 wt.%CaO for foam stabilisation. They also confirm the formation of MgO due to the decomposition of $CaMg(CO_3)_2$and its action as foam stabilising agent. The present authors in

their previous work successfully demonstrated foaming aluminium scrap alloys using TiH_2 as blowing agent [12]. Here, the stable oxide covers on the swarf which were trapped as bi-films during melting act as stabilising particles in foams. The stabilisation behaviour of these oxide (Al_2O_3) bi-films during foaming in the presence of various amounts of Mg (added for 'conditioning' the scrap alloy) is investigated in the present paper.

2. Experimental Procedure

2.1 Alloy preparation

The scrap used was mm-sized chips, a by-product of the machining of LM26, an Al-Si alloy commonly used for making automotive castings. Their morphology is shown in Fig.1 and the approximate composition as measured by optical emission spectroscopy (OES) is given in Table 1 where it can be seen that there is 0.13 wt.% Mg in the ingot-derived base alloy. The as-received scrap, which had already been roasted at ~400 °C to remove residual oil and cutting lubricants, was additionally heat-treated at 500 °C in air for 24 h in an effort to increase the oxide content.

Processing of the scrap into ingots was performed by charging a crucible (preheated to 750 °C) with scrap. After melting of the scrap (which takes roughly 30 min) the charge needed to be vigorously stirred to amalgamate the individual molten chips. Given the poor packing of the chips, this produced only a partially filled crucible, which is why the procedure was repeated twice to produce a full charge. After the final addition and stirring, 0, 1 or 2 wt.% Mg additions were introduced via an Al-25 wt.%Mg master alloy, after which the melt was kept at temperature for 4 h for "conditioning". After this final step, the metal was briefly stirred and then cast into a steel mould.

2.2 Relative viscosity measurement

The torque required to stir the molten scrap alloys was measured using an apparatus resembling a concentric cylinder viscometer. In this arrangement, a 70 mm outer diameter (OD) graphite bob was rotated at 1000 ± 5 rpm in a cylindrical crucible with an internal diameter of 87 mm. The melt temperature was held at 700 ± 2 °C and the volume of metal and bob immersion depth were kept constant. The stirring torque was measured (at a rate of 0.2 Hz for periods up to 1 h) using a Heidolph RZR 2102 overhead stirrer capable of measurement (in N.cm) to 4 decimal places. Prior to each measurement the stirrer was warmed-up for 30 min by stirring the empty assembly at temperature, giving a baseline reading prior to the measurement with alloy in the crucible. Since for this type of setup the stirring torque is directly proportional to the viscosity, expressing the torque relative to that required to stir the ingot-derived base alloy will enable the fractional changes in viscosity as a function of scrap and elemental additions to be determined.

2.3 Foaming process

Foaming was performed by an interrupted foaming process which is analogous to what is termed the "Formgrip" method in the literature[13].This method consists of two stages in the preparation of foams. In the first stage, 100 g of composite was melted in an alumina crucible inside a furnace at 700 °C. After the melt had reached the desired temperature,1.5 wt.% of treated TiH_2 powder (pre-oxidised in air for 24 h at 400 °C and 1 h at 500 °C) was admixed and stirred for 60 s with a graphite stirrer rotating at 600 rpm. The advantage of using treated TiH_2 is the development of a surface oxide layer on each TiH_2 particle which slows the decomposition rate of the metal hydride during foam processing, helping in the effective preparation of foamable precursors. Immediately after mixing, the melt was rapidly quenched by pouring it into a water-cooled copper mold of 25 mm diameter

and 100 mm height to obtain high density castings. Subsequent to this, these castings were sliced in the transverse direction to obtain the desired weight of the foamable precursor and foamed separately.

The foaming trials were performed under ambient atmosphere and pressure. For each sample type, three identical samples (each 4.5 g) were foamed by heating on a resistive heating plate on a faster heating rate to 750 °C within 60 s and holding there for 600 s. After this, the heater was turned off and natural cooling took place. The sample temperature was measured by a thermocouple fed through a hole in the bottom of the heating plate. Foam evolution was monitored in-situ by an X-ray radioscopy set-up comprising a micro-focus X-ray source and a panel detector as described in Ref. [14]. In this work, the X-ray spot size was set to 5 µm applying 100 kV voltage and 100 µA current. A series of X-ray projected images of the foaming samples were obtained and analysed with the dedicated software AXIM[15]. Expansion was measured in terms of the growth of the projected volume of the sample.

2.4 Microstructural and compositional analysis

The oxygen content in the chips and in the resulting cast alloys was measured using a LECO TC-436AR analyser, which enables oxygen content measurement (in wt.%) to be measured to 3 decimal places. XRD of the alloys was performed using Cu-Kα radiation. The base alloys and cross sections of foams were metallographically polished and electropolished using a mixture of orthophosphoric acid, ethanol and water as the electrolyte. The polished samples were observed using an optical and a high-resolution scanning electron microscope.

3. Results

3.1 Composition and microstructure of the base alloy

The oxygen content measured in the as-received swarf was 0.11 ± 0.01 wt.%, increasing to 0.53 ± 0.05 wt.% after heat treatment. If we assume that all the oxygen is contained in Al_2O_3, this corresponds to 0.23 and 1.13 wt.% Al_2O_3, respectively. Typical oxygen levels in the corresponding base alloy were < 0.03 wt.%. Since the loose swarf is heated over a prolonged period in the crucible, the oxygen level in the cast re-melted scrap alloy was also measured and found to be 0.60 ± 0.07 wt.% (1.27 wt.% Al_2O_3).

Figure 2 shows X-ray diffraction on re-melted scrap alloys containing different levels of Mg addition. It shows the presence of $MgAl_2O_4$ (spinel) and MgO even in the case when no Mg has been added. There are no significant changes in the intensity of the $MgAl_2O_4$ and MgO peaks for the alloys containing added Mg, but the formation of transition phases and Mg_2Si is readily detected and found to increase in proportion with increasing Mg addition.

Figure 3 shows optical micrographs of oxide films and clusters in the scrap alloys that originate from the surfaces of the chips and the effect of Mg addition. It is apparent from these images that the oxide clusters, although highly variable in size and shape, are larger in the alloy to which no Mg has been added (typically >400 μm in diameter) and that, whilst some large clusters still persist, they become smaller and more uniformly dispersed after Mg addition Figures 4a-d show SEM images of typical oxide films and clusters in the metallographically polished and electro-polished conditions. A closer look at the oxides in the electro-polished section shows that the oxides are highly tangled thin sheets. Figures 4c and d show ultra-fine (< 1 μm) particles present on the oxide surface in an alloy sample containing 1 wt.% Mg. The octahedral morphology (Fig. 4d) and the Mg, Al and O peaks seen in the energy dispersive X-ray spectrum shown in Figure 4e confirm that the particles are $MgAl_2O_4$ (spinel). For stoichiometric spinel, i.e. $MgAl_2O_4$,the Al/Mg ratio is equal to 2 (the oxygen composition from EDS can be ignored). MgO is present as fine nm-sized needle

shaped particles as shown in ref. 8 &16 which are difficult to identify in the present sample microstructure.

3.2 Relative viscosity of the base alloys

Figure 5a shows typical plots for the stirring torque (in this case for the scrap with no Mg addition and for the ingot-derived base alloy, after the subtraction of the baseline torque for rotating the paddle in an "empty" system, as a function of stirring time. The torque is constant with time over the 1 h measurement period with average torque values of 1.43 N.cm and 0.71 N.cm for the scrap and base alloy, respectively. Figure 5b displays the average stirring torque for the various alloys as a function of Mg content, normalised with respect to the ingot-derived base alloy to give a measure of the relative viscosity. For the re-melted scrap the relative viscosity increases, which is similar to what has been observed by other researchers when adding "thickeners" to produce Al foams [17], but is below the typical five-fold increase observed for Ca additions to Al in the Alporas process [18]. Addition of 1.0 and 2.0 wt.% Mg to the re-melted scrap reduces the relative viscosity to 1.83 N.cm and 1.76 N.cm, respectively, a larger decrease than observed when adding 2 wt.% Mg to the ingot-derived base alloy (0.96 N.cm).

3.3 In-situ foaming

The in-situ foaming under X-ray radioscopy shows (Fig. 6a-c) the foam evolution as a function of time. Without Mg addition (Fig. 6a) the foam reaches its maximum expansion within a shorter period (60 s) and steadily collapses during subsequent isothermal holding and again when solidifying. Addition of Mg decreases the expansion rate but the foam continues to expand until the end of the experiment (600 s). The volume expansion vs. time

plot (Fig. 6d) confirms the result of radioscopy and from this it is apparent that the alloy with 1 wt.% Mg addition shows the maximum expansion after 600 s holding.

3.4 Foam microstructures

The SEM images in Fig. 7a and b show the rough cell wall surface for a foam without added Mg, where oxide films or clusters protrude into the gas phase. An EDX spectrum (Fig. 7c) of the protruding oxide shows Al and O peaks confirming that the particle is Al_2O_3. The addition of 1 wt.% Mg (Fig. 8a-c) results in much smoother cell wall surfaces with far fewer protruding oxides. The growth of additional nodular phases on these protuberances is also apparent. Smooth cell wall surfaces can also be seen on the foam with 2 wt.%Mg addition (Fig. 9a and b) with high levels of nodular growth covering the cell wall surface. The EDX spectrum (Fig. 9c) of a protruding oxide shows Al, Mg and O peaks, evidence for the presence of Mg-Al-O type of oxide.

4. Discussion

Heat treatment of the chips and exposition to the environment during melting both contribute to an increase in the oxide content and therefore the thickness of the oxide layer on the surface of the chips. Melting these chips produces a charge that requires fairly vigorous stirring to bring the individual chips together and to produce a viscous liquid due to the resilience of the oxide films that encapsulate the molten chips, a behavior that is similar to that observed when melting aluminium powder [19].

XRD clearly indicates the presence of $MgAl_2O_4$ (spinel) and MgO in the base alloys. It is reported [20] that a low concentration (0.02 wt.%) of Mg in the melt can readily destabilize Al_2O_3 to form $MgAl_2O_4$ and even higher concentration (>0.06 wt.%) of Mg yields MgO at 1000 K (727 °C). The possible reactions as given in Ref.19 are:

$$3Mg_{(l)} + 4\ Al_2O_3 \rightarrow 3MgAl_2O_{4(s)} + 2\ Al_{(l)}$$

$$\Delta F_{1000K} = -76.6\ kJ.mol^{-1} \quad (1)$$

$$MgO_{(s)} + Al_2O_{3(s)} \rightarrow MgAl_2O_{4(s)}$$

$$\Delta F_{1000K} = -47\ kJ.mol^{-1} \quad (2)$$

It is clear that lower Mg levels (~1 wt.% and below) will favour the formation of $MgAl_2O_4$, with the formation of MgO above this level and a wide compositional range in which $MgAl_2O_4$ and MgO coexist [21-25].

The Mg contents in the alloys in this study would enable either 14% of the oxide to be converted to MgO or 58% to $MgAl_2O_4$ in the case of the alloy to which no extra Mg was added, but full conversion in both the others (with >1 wt.% excess for 2 wt.% addition). These values are the maximum possible in the unlikely case that no further Mg loss occurred during melt processing. Predicted oxide levels are either 1.5 wt.% or 1.35 wt.% based on complete conversion of the 0.60 wt.% oxygen (or 1.27 wt.% Al_2O_3) to MgO or $MgAl_2O_4$, respectively. These oxide levels are considerably higher than those that are thought to be optimum for good expansions in foams made by a powder route, which are typically up to 0.3 to 0.6 wt.% [4, 26].

Irrespective of the compound formed, it is expected that wetting of the Al_2O_3 films is improved by the reaction of Mg in molten Al [8,23,25] and that reaction and the volume expansions associated with these reactions or the porous reaction products that form cause embrittlement and cracking of the oxide films [21,24,27].These processes contribute, in conjunction with stirring, to the fragmentation of the large oxide clusters, their improve dispersion in the liquid and, in combination with the inherent (albeit fairly small) reduction in viscosity with Mg addition,a decrease in viscosity of the re-melted scrap is observed with increasing Mg content.When measuring the stirring torque for pre-prepared alloys it was

constant throughout the 60 min stirring period, indicating that any reactions affecting the viscosity had already occurred during the "conditioning" period.

The formation of $MgAl_2O_4$ or MgO observed qualitatively through the microstructure seems to be not as pronounced as reported in Ref. [8]. This is due to the sluggish reaction of Al_2O_3 with Mg in comparison to other oxides such as SiO_2[16]. The $MgAl_2O_4$ particles grown at the surface of the Al_2O_3 films of 100 µm size looks similar to the formation of $MgAl_2O_4$ on the surface of quartz (SiO_2) particles as shown in ref. 8

The alloy foams derived from scrap with added Mg can be compared in terms of their expansion and stability with the powder-processed AlSi9Cu3 foam [11] and the vacuum-compacted binary AlSi11 foam [28], since in both the processes aluminium oxides act as stabilizing agents. The expansion of the scrap alloy foam with no Mg addition is rapid, which is not comparable with any other foam, but the steady collapse on holding (600 s) is similar to the foams produced through powder route [29-32]. From the in-situ investigation it is clear that the morphology and homogeneity of bubbles and the overall expansion and stability of the scrap alloy foams with 1 and 2 wt.% Mg addition is comparable with Alporas [33] and Formgrip foams [13] where CaO and SiC particles, respectively, are used as stabilizing agent.

The in-situ foaming experiments show that whilst Mg additions do not increase the expansion within the period of observation, they greatly improve foam stability. It is thought that the large native oxide clusters are unable to stabilise the foam over a long time, as they do in the first seconds of foaming due to their highly tangled structure and poor wettability with molten aluminium, leading to drainage of liquid and foam collapse. It is only through the reaction that forms $MgAl_2O_4$ or MgO on their surfaces and their improved wetting with respect to the liquid that they can become effective for stabilization. This results in little or no drainage of liquid through the foam structure[8, 34,35].

The enhanced efficiency of particles in stabilizing foam is reflected by the change in their location in the cell wall structure. With poor wetting the oxides are mostly found protruding into the gas phase, which gives the cell wall a rough appearance. When wetting is improved through reaction the particles are retained within the cell walls, which give them a much smoother appearance (this process is shown schematically in Fig.10).

The stabilisation mechanism is thought to be shared with foams made by a powder route, where the dispersed oxide films increase the bulk viscosity and form networks that are barriers to the passage of the melt, slowing down the vertical motion of liquid metal induced by drainage [4,36]. Although the addition of Mg was observed to decrease the bulk melt viscosity, it is thought that the resultant formation of wetted oxides at the liquid-gas interface will increase the surface viscosity, inhibiting the flow of liquid, thereby improving the stability of the foam structure. In the same way this increase in the surface viscosity would account for a slowing down of foam expansion compared to the alloys with no added Mg.

The decreasing trend of normalised torque of the swarf melt with an increase in Mg addition as seen in Fig. 5b is unexpected since Mg addition to aluminium is supposed to increases the melt viscosity [20]. In the present study, the decrease in the bulk melt viscosity of the scrap alloy with increasing Mg addition can be attributed to the morphology of oxides, which are in the form of highly tangled sheets. This morphology aids an easy distribution in the melt and therefore improves its shearability [37]. Foaming would have been impossible if the oxides present in scrap alloys were finer such as in the foams made from powders [36]. This could be attributed to larger surface area of the finer particles which would enhance the Mg reaction and therefore severely increases the melt viscosity

Although it is likely that there are traces of Mg even in the base alloy and there is evidence of a partial reaction of the oxide, the extent to which this reaction occurs appears to be insufficient to encourage sufficient wetting or wetting of a significant fraction of the

oxides to facilitate foam stabilisation. With 1 wt.% Mg addition, complete conversion of the oxide is possible and with 2 wt.% of Mg, more than 1 wt.% Mg will be in excess, thus affecting the melt viscosity. A similar addition of 1 wt.% Mg reduces the surface tension of aluminium sharply (from 0.860 N/m to 0.650 N/m). Upon further increase of the Mg addition above 1% the reduction of surface tension is marginal [20]. The enhanced surface wetting of the oxides due to the reaction with Mg is the reason for the enhanced stability and expansion in these foams.

5. Summary

1. Aluminium alloys made from machining chips that have been heat treated and re-melted have been successfully foamed after the addition of TiH_2.
2. Through additional alloying with Mg foams with low densities (< 0.3 g/cm^3), good stability in the liquid state and good pore structures were obtained.
3. Foam formation and stabilisation is possible through the introduction of oxide films associated with the scrap.
4. Although the tendency for these oxides is to form clusters, by alloying with Mg (1 wt.% and 2 wt.%) and holding in the liquid state to allow reactions to take place fragmentation and wetting of the oxides occurs. The enhanced wetting of the particles is due to the reaction products, namely $MgAl_2O_4$ and MgO that form on the surface of the oxides. Therefore, the stability and expansion of the foams increases. The decrease in expansion and increased stability of foams containing 1 wt.% or 2 wt.% Mg when compared to foams with no Mg addition can be attributed to the increase in the surface viscosity.

References

1. Banhart J (2001) Manufacture, Characterisation & application of cellular metal & metal foams, Prog Mater Sci 46: 559-632.
2. Drenchev L, Sobczak J, Malinov S, Sha W (2006) Gasars: A class of metallic materials with ordered porosity, Mater Sci Technol 22: 1135-1147.
3. Ip S, Wang Y, Toguri J (1999) Aluminum foam stabilization by solid particles, Can Metall Q 38:81-92.
4. Banhart J(2000) Manufacturing routes for metallic foams. JOM 52: 22-27.
5. Babcsán N, Leitlmeier D, Degischer H.-P (2003)Foamability of particle reinforced aluminum melt, Materialwissenschaft und Werkstofftechnik 34: 22-29.
6. Babcsán N, Garcia-Moreno F , Banhart J (2007) Metal foams-High temperature colloids: Part II: In situ analysis of metal foams, Colloids Surf A 309: 254-263.
7. Babcsán N, Vinodkumar G S, Murty B S, Banhart J (2007) Grain Refiners as Liquid Metal Foam Stabilisers, Trans Indian Inst Met 60:127-132.
8. Vinod Kumar G S, Chakraborty M, Garcia-Moreno F , Banhart J (2011) Foamability of $MgAl_2O_4$ (Spinel)-Reinforced Aluminum Alloy Composites, Metall Mater Trans A 42: 2898-2908.
9. Kanetake N, Kobashi M, Tsuda S(2008) Foaming behavior of aluminum precursor produced from machined chip waste, Adv Eng Mater 10: 840-844.
10. Ha W, Kim S K, Jo H.-H, Kim Y.-J (2005) Optimisation of process variables for manufacturing aluminium foam materials using aluminium scrap. Mater Sci Technol 21: 495-499.
11. Haesche M, Lehmhus D, Weise J, Wichmann M, Mocellin I C M (2010)Carbonates as foaming agent in chip-based aluminium foam precursor, J Mater Sci Technol 26: 845-850.

12. Vinodkumar G S, Heim K, Garcia-Moreno F, Banhart J, Kennedy A.R (2013) Foaming of Aluminum Alloys Derived From Scrap, Adv Eng Mater 15: 129–133.

13. Gergely V,Clyne B (2000) The FORMGRIP process: Foaming of reinforced metals by gas release in precursors, Adv Eng Mater 2: 175-178.

14. Garcia-Moreno F, Babcsán N, Banhart J (2005) X-ray radioscopy of liquid metalfoams: Influence of heating profile, atmosphere and pressure, Colloids Surf A 263: 290-294.

15. Garcia-Moreno F, Fromme M, Banhart J (2004) Real-time X-ray Radioscopy on Metallic Foams Using a Compact Micro-Focus Source, Adv Eng Mater 6: 416-420.

16. Sreekumar V M, Pillai R M, Pai B C, Chakraborty M (2008) Evolution of $MgAl_2O_4$ crystals in Al-Mg-SiO_2 composites. Appl Phys A 90: 745-752.

17. Yang C, Nakae H (2003)The effects of viscosity and cooling conditions on the foamability of aluminum alloy. J Mater Process Technol 141: 202-206.

18. Ma L, Song Z (1998) Cellular structure control of aluminium foams during foaming process of aluminium melt, Scrip Mater 39: 1523-1528.

19. Babcsán N, Garcia-Moreno F, Banhart J (2007) Metal foams- high temperature colloids part II: in-situ analysis of metal foams, Colloids Surf A 309: 254–263

20 Pai B C, Geetha Ramani, Pillai R M, Satyanarayana K G (1995) Role of magnesium in cast aluminium alloy matrix composites, J Mater Sci 30: 1903-1911.

21. Sreekumar V M, Pillai R M, Pai B C, Chakraborty M (2008) A study on the formation of $MgAl_2O_4$ and MgO crystals in Al–Mg/quartz composite by differential thermal analysis, J. Alloys Compd 461: 501-508.

22. Xie G, Ohashi O, Yamaguchi N, Song M, Mitsuishi K, Furuya K, Noda T (2003) Behavior of oxide film at interface between particles of Al-Mg alloy powder

compacts prepared by pulse electric current sintering, Jpn. J. Appl. Phys 42: 4725-4728

23. Schaffer G, Sercombe T, Lumley R (2001) Liquid phase sintering of aluminium alloys, Mater Chem Phys 67: 85-91.

24. Hanabe M, Aswath P (1997) Synthesis of in-situ reinforced Al composites from AlSiMgO precursors. Acta Mater 45: 4067-4076.

25. McLeod A, Gabryel C (1992) Kinetics of the growth of spinel, $MgAl_2O_4$, on alumina particulate in aluminum alloys containing magnesium. Metall Trans A 23:1279-1283.

26. Asavavisithchai S, Kennedy A R (2006) Effect of powder oxide content on the expansion and stability of PM-route Al foams. J Colloid Interface Sci 297: 715-723.

27. Lumley R, Sercombe T, Schaffer G (1999) Surface oxide and the role of magnesium during the sintering of aluminum, Metall Mater Trans A 30: 457-463.

28. Jiménez C, Garcia-Moreno F, Mukherjee M, Goerke O, Banhart J (2009) Improvement of aluminium foaming by powder consolidation under vacuum, Scrip Mater 61: 552-555.

29. Duarte I, Banhart J (2000) A study of aluminium foam formation kinetics and microstructure, Acta Mater 48: 2349–2362

30. Duarte I, Oliveira M, Garcia-Moreno F, Mukherjee M, Banhart J (2013) Foaming of AA6061 using multiple pieces of foamable precursor, Colloids Surf A 438: 47– 55

31. Mukherjee M ,Garcia-Moreno F, Banhart J (2010) Collapse of Aluminium foam in two different atmosphere, Metall Mater trans B 41: 500-504

32. Garcia-Moreno F, Mukherjee M, Jiménez C, Rack A, Banhart J (2012) Metal foaming investigated by X-ray radioscopy, Metals 2: 10-21

33. Miyoshi T, Itoh M, Akiyama S, Kitahara A (2000) ALPORAS aluminum foam: production process, properties, and applications. Adv Eng Mater 2: 179-183.

34. Sangghaleh A, Halali M (2009) Effect of magnesium addition on the wetting of alumina by aluminium, Appl Surf Sci 255: 8202-8206.

35 Asavavisithchai S, Kennedy A R (2006) The effect of Mg addition on the stability of Al-Al_2O_3 foams made by a powder metallurgy route. Scrip Mater 54: 1331-1334.

36. Körner C, Arnold M, Singer R F (2005) Metal foam stabilization by oxide network particles. Mater Sci Eng A 396: 28-40.

37. Fan Z (2002) Semisolid Metal Processing, Int Mater Rev 47: 49-85

Figure
Click here to download Figure: foaming scrap alloy_figures_final.docx

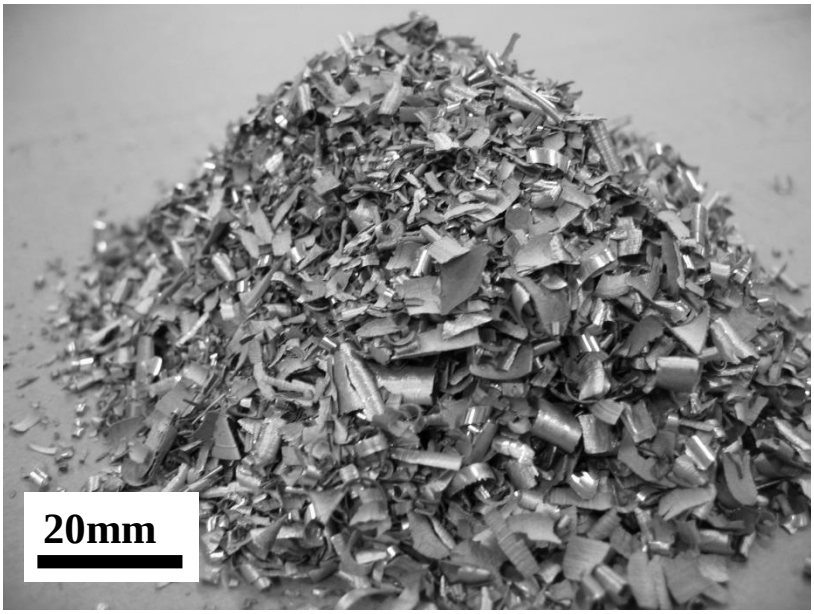

Fig.1 Morphology of the machining (swarf) chips.

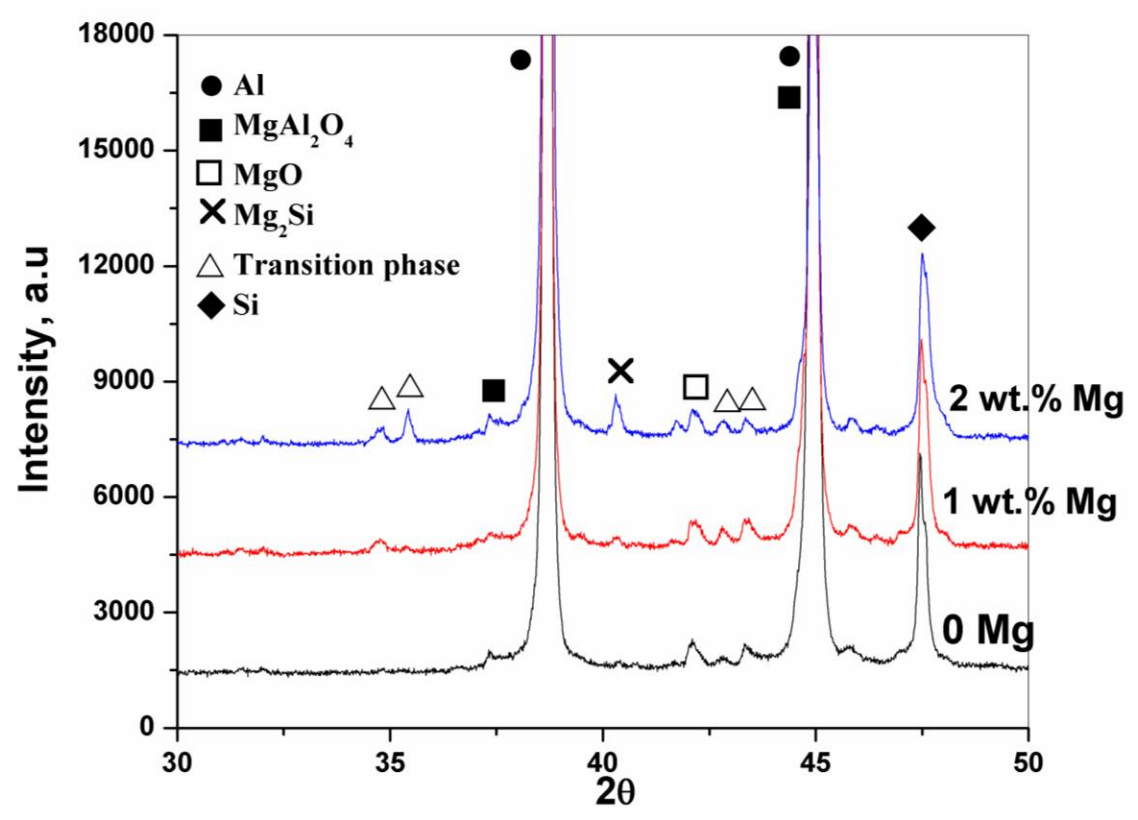

Fig. 2 XRD plots of remelted and solidified scrap (LM26, Al-Si-Mg) with and without Mg addition.

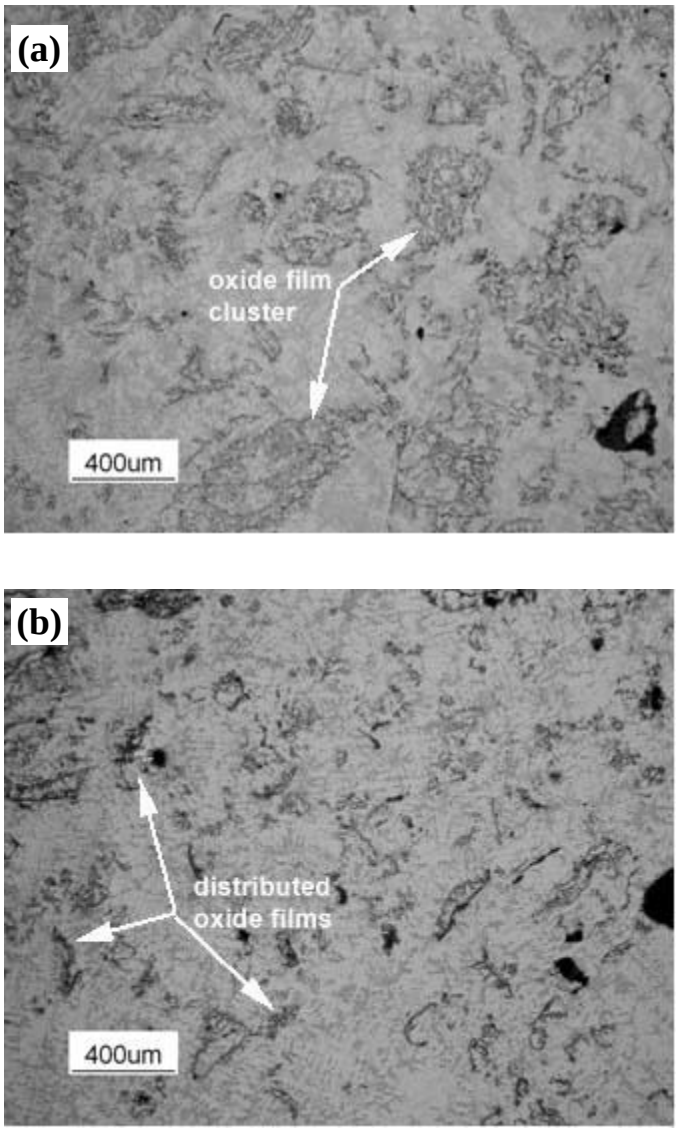

Fig.3 Optical micrographs of oxide films and clusters in (a) a re-melted and solidified scrap alloy and (b) the same but with 2 wt.% Mg addition.

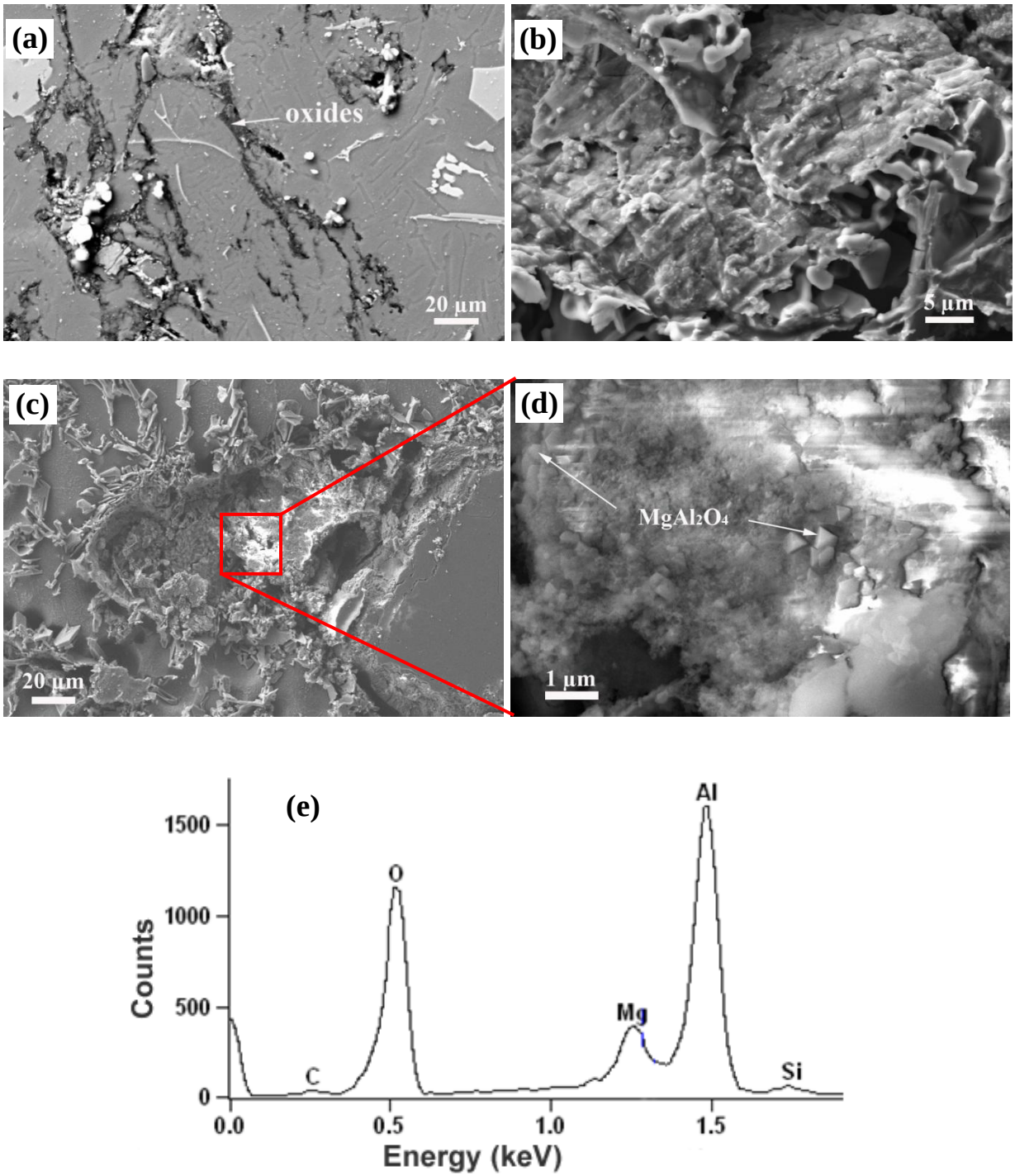

Fig.4 SEM micrographs of (a) and (b) oxide bi-films in re-melted and solidified scrap alloys, electro-polished surface investigated. (c) and (d) oxides in an alloy containing 1 wt.% Mg and reaction products with an octahedral morphology. (g) EDX spectrum of one of these octahedral particles.

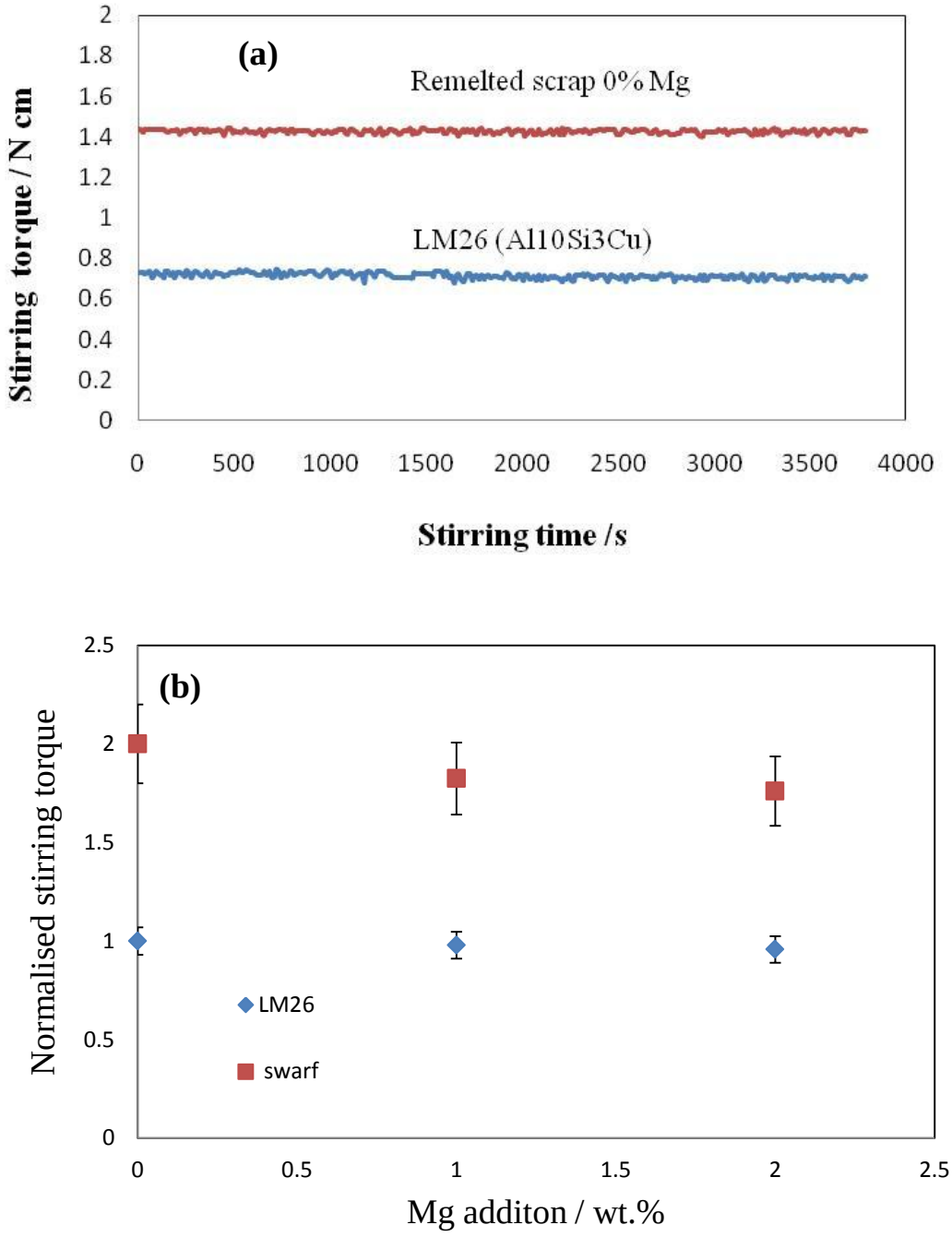

Fig.5 Stirring torque as a function of time (a) for remelted scrap and (b) stirring torque as a function of Mg addition, normalised with respect to the ingot-derived base alloy.

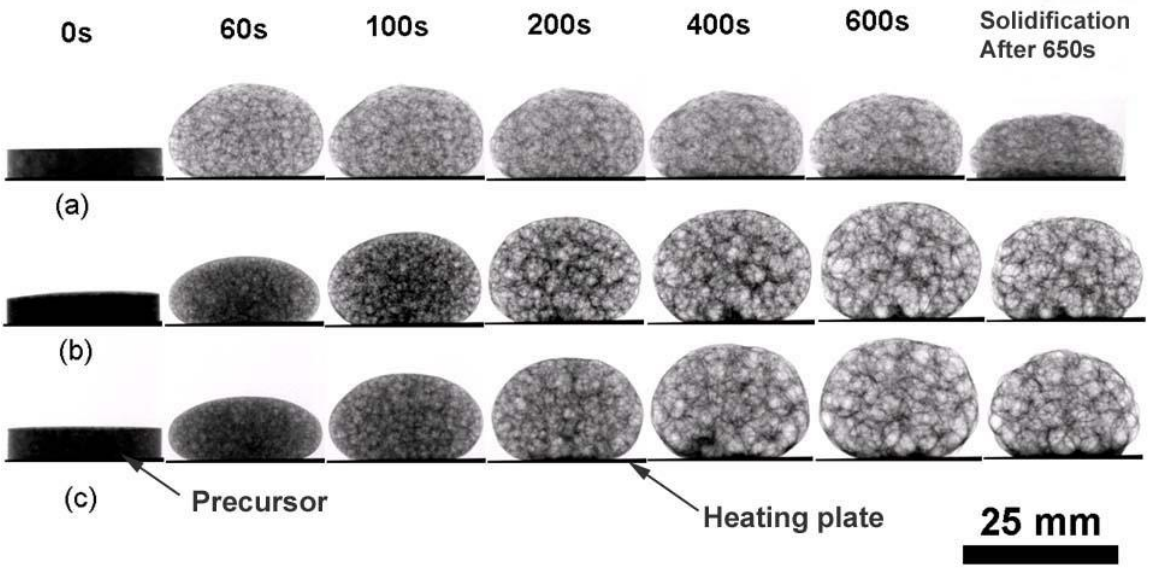

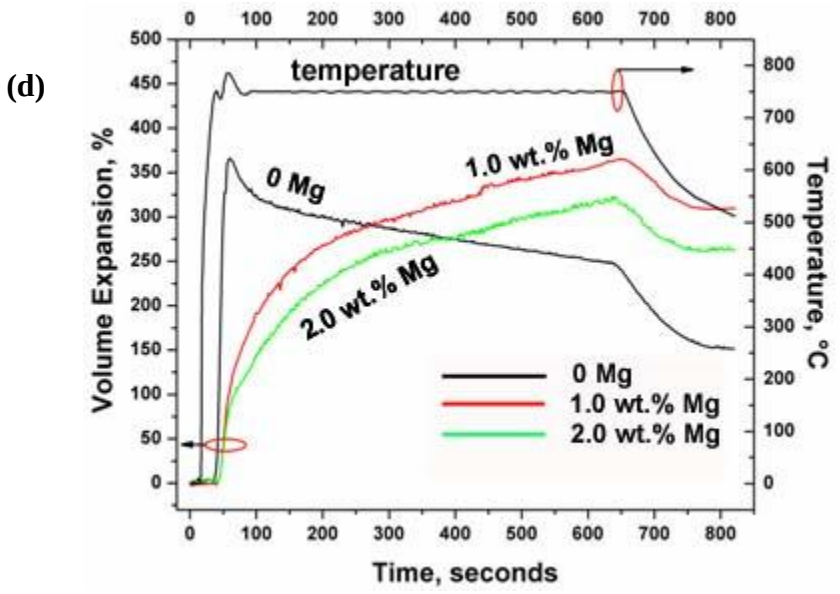

Fig.6 In-situ X-ray radioscopy of evolution of foam made from remelted scrap. (a) 0 wt.% Mg, (b) 1 wt.% Mg and (c) 2 wt.% Mg and (d) volume expansion of the foams as a function of time.

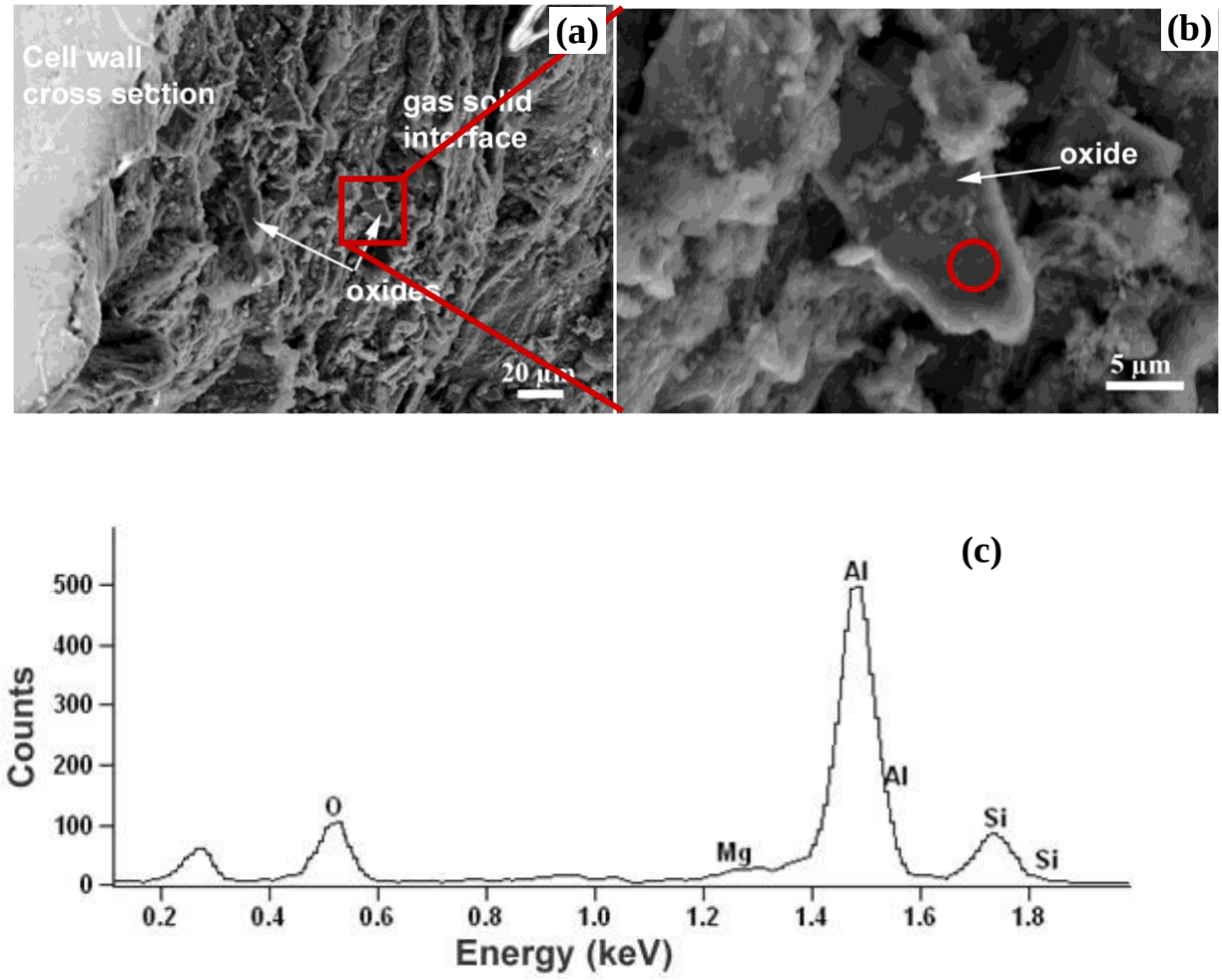

Fig.7 SEM micrographs showing(a) the inner surface of the cell wall of a foam made from remelted scrap with no added Mg and (b) a magnified section of (a). The red circle in the micrograph (b) indicates the spot where EDX has been taken. (c) EDX spectrum showing Al, Mg and O peaks.

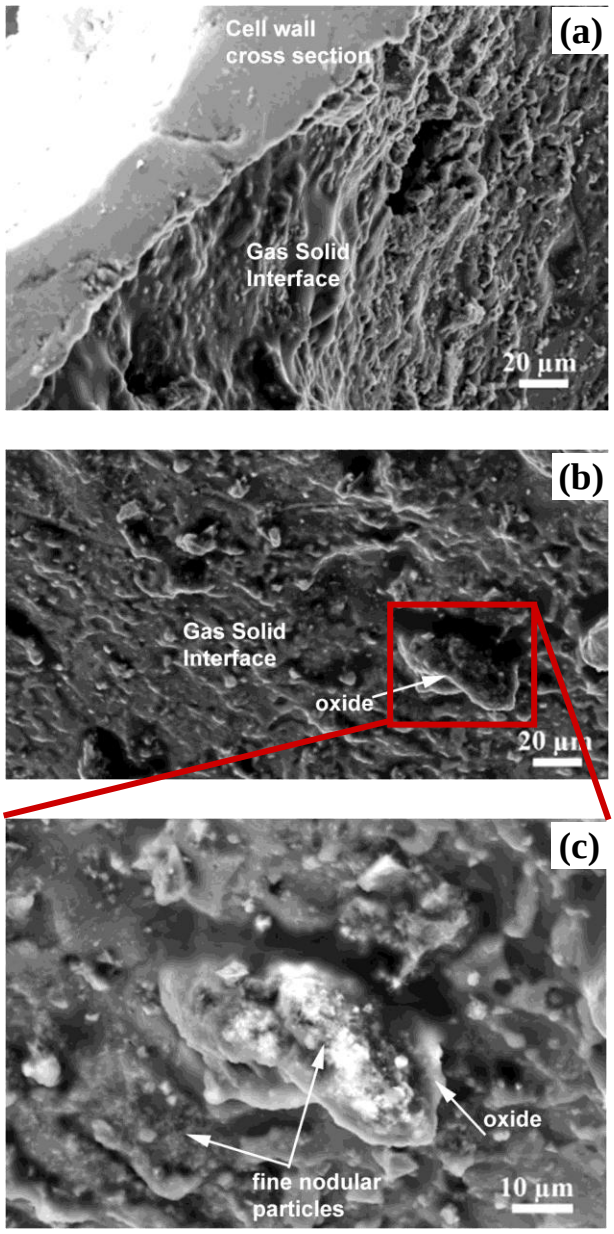

Fig.8 SEM micrograph of the inner surface of a cell wall of a foam made of remelted scrap containing added 1 wt.% Mg showing (b) and (c) a protruding oxide particle at the gas-solid interface and fine reaction products on the surface.

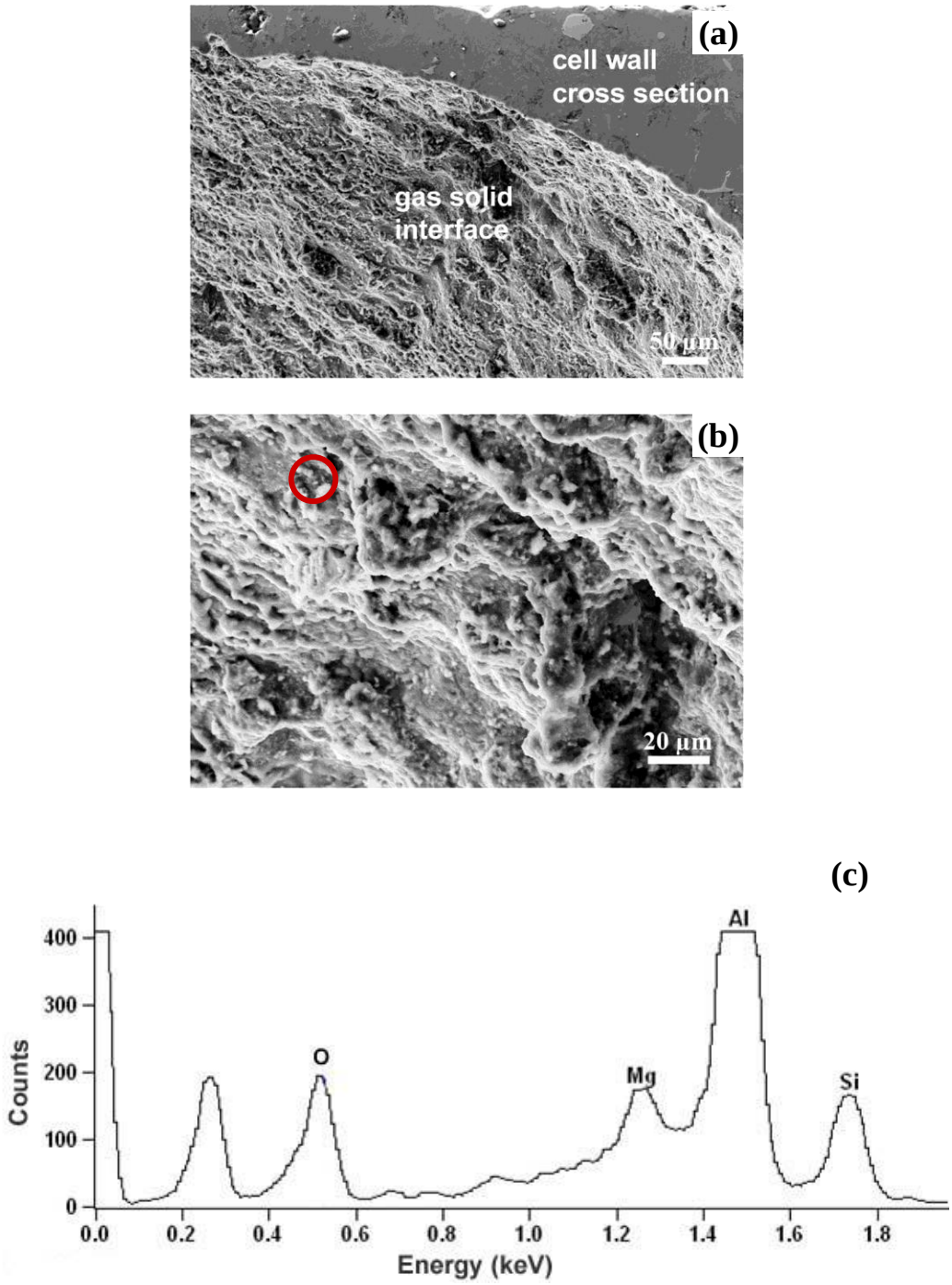

Fig.9 SEM micrograph of the inner surface of a cell wall of a foam containing 2 wt.% Mg, showing (b) extensive oxide coverage.(c) EDX analysis of this oxide layer. The red circle in the micrograph (b) indicates the spot where EDX has been taken.

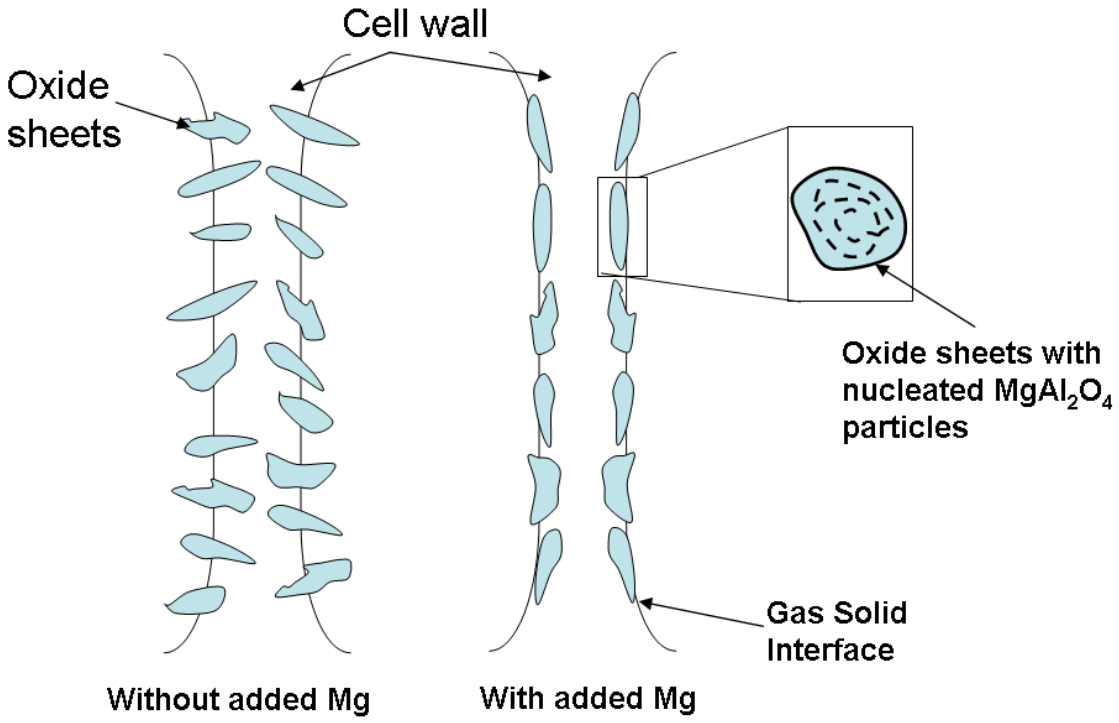

Fig.10 Schematic of oxide cluster location in the cell walls, with and without added Mg. Particles protrude into the gas phase in the absence of Mg. With Mg addition, the oxide clusters are located within the cell walls.

Table
Click here to download Table: Foaming scrap alloy_table.docx

Table 1. Chemical composition of the machining chips as measured by OES.

Element	Si	Cu	Fe	Mn	Mg	Zn	Al
wt.%	10.50	1.60	1.20	0.29	0.13	1.10	balance